BMC Chemistry

RESEARCH Open Access

In silico estimation of polyethylene glycol coating effect on metallic NPs radiosensitization in kilovoltage energy beams

Elham Mansouri[1,2], Saeed Rajabpour[3] and Asghar Mesbahi[3*]

Abstract

Purpose Nanoparticles (NPs) as radiosensitizers present a promising strategy for enhancing radiotherapy effectiveness, but their potential is significantly influenced by the properties of their surface coating, which can impact treatment outcomes. Most Monte Carlo studies have focused on metallic NPs without considering the impact of coating layers on radiosensitization. In this study, we aim to assess both the physical and radiobiological effects of nanoparticle coatings in nanoparticle-based radiation therapy.

Materials and methods In this simulation study, we used Geant4 Monte Carlo (MC) toolkit (v10.07.p02) and simulated the bismuth, gold, iridium and gadolinium NPs coated with polyethylene glycol (PEG-400: Density: 1.13 g/cm^3, Molar mass: 380–420 g/mol) as radiosensitizer for photon beams of 30, 60 and 100 keV. Secondary electron number and reactive oxygen species enhancement factor were estimated. Also, dose enhancement factor (DEF) was determined in spherical shells with logarithmic scale thickness from the nanoparticle surface to 4 mm.

Results Secondary electron emission was highest at 30 keV for gold, bismuth, and iridium NPs, while gadolinium NPs peaked at 60 keV. Coating reduced electron emissions across all energies, with thicker coatings leading to a more significant decrease. DEF values declined with increasing radial distance from the NP surface and were lower with thicker coatings. For gadolinium NPs, DEF behavior differed due to K-edge energy effects. Reactive species generation varied, showing maximum production at 30 keV for gold, bismuth, and iridium NPs, while gadolinium NPs showed peak activity at 60 keV. PEG coatings enhanced reactive species formation at 100 keV.

Conclusion The findings indicate that the coating layer thickness and material not only influence the emission of secondary particles and DEF but also affect the generation of reactive species from water radiolysis. Specifically, thicker coatings reduce secondary particle emission and DEF, while PEG coatings demonstrate a dual behavior, offering both protective and enhancing effects depending on photon energy. These insights underscore the importance of optimizing NP design and coating in future studies to maximize therapeutic efficacy in nanoparticle-based radiation therapy.

Keywords Monte Carlo, Radiosensitization, Coating, Nanoparticle

*Correspondence:
Asghar Mesbahi
amesbahi2010@gmail.com
[1]Student Research Committee, Tabriz University of Medical Sciences, Tabriz, Iran
[2]Drug Applied Research Center, Tabriz University of Medical Sciences, Tabriz, Iran
[3]Medical Radiation Sciences Research Center, Tabriz University of Medical Sciences, Tabriz, Iran

Introduction

High-density metallic nanoparticles (NPs) combined with low-energy external beam X-rays or brachytherapy sources could significantly enhance the delivered dose and tumor controlling parameters could be enhanced and reducing side effects in healthy tissue surrounding the cancerous region [1, 2]. Researchers have utilized various Monte Carlo (MC) codes, with studies reporting physical dose enhancement around metallic NPs when exposed to different radiation sources such as X-rays, electron and proton beams [3–22].

Secondary electrons and photons released from an exposed metallic surface are the cause of sensitization. Nanodosimetric characteristic of high-Z metallic NPs could significantly increase the local dose and lethal effect of irradiation through photoelectric effect followed by the emission of Auger electrons and electrons induced by X-ray fluorescence. The radiosensitizing effect of metallic NPs is partly due to their ability to emit large quantities of secondary electrons upon irradiation. This effect is particularly pronounced for kilovolt photon beams around 100 kVp, where dose enhancement primarily results from low-energy secondary electrons, such as Auger electrons, which have a limited range [23–25]. Nanoscopic dose enhancement has been demonstrated to have a significantly greater biological impact compared to macroscopic dose enhancement [26]. It is well known merely in the case of keV photons, biological consequences of nanoparticle radiosensitization are primarily associated with the outcomes of the photoelectric interactions between photons and matter. Interaction of nanoparticle with the incident photon result in the emission of secondary electrons and photons.

For biomedical applications, NPs are often coated with organic materials to enhance stability in physiological environments and minimize potential toxic biological effects [27]. Also nanoparticle coating could be applied for tumor selecting [28]. Polymers can serve as soft tissue substitutes and could be used as biodegradable biomaterials in clinic [29, 30]. It has been shown that Coating of metallic NPs with poly ethylene glycol (PEG) could increase the probability of reaching of nanoparticle to the tumor and could cause longer blood circulation time Surface modification may influence the spectral characteristics of generated secondary electron [31]. The physicochemical features of coated NPs could be influenced based on the nature of the coating substance and its thickness. Coating layer could stop and absorb a portion of generated low-energy, short-range electrons, reducing the delivered dose and energy to the surrounding medium. Free radicals are largely responsible for the majority of biological damage resulting from ionizing radiation. Also, the coating layer could influence the production of radicals and affect the radiosensitizing potential of the coated metallic NPs. This effect could be related to the water content of coated layer and physical interaction of radiation with nanoparticle and coating layer. MC simulation codes at the microscopic and nanoscopic scales utilize the technique known as "trace structure. Geant4-DNA incorporates chemical, physical, and biological models to effectively simulate cellular and subcellular damage caused by ionizing radiation. In the current study, Geant4 were performed to investigate the macroscopic and microscopic dose enhancement effect of PEG coated bismuth, gold, iridium and gadolinium NPs. Most previous studies have focused on the coating layer's characteristics for minimizing the toxicity of nanoparticles (NPs) and enhancing their stability and biocompatibility. While the radio-enhancement potential of coated NPs has been validated by several investigations, the primary emphasis has been on reducing toxicity, improving stability, and ensuring biocompatibility. However, the absorptive effects of the coating layer have often been overlooked and not adequately addressed. By examining how coating layers can function as a protective shield for nanoparticles (NPs) and influence the dose enhancement factor during radiotherapy, this work paves the path to developing more targeted and effective treatment methods in the future. The study highlights the need to consider both the biological and physical impacts of coating thickness in nanoparticle-based radiation therapy, highlighting its importance in advancing cancer treatment strategies. The results presented herein give a physical and biological view of radiosensitization potential of different metallic NPs and if the coating layer of NPs with different thickness could influence the physical and biological dose enhancement of NPs.

Materials and methods

The Geant4 v10.07.p02 open-source and general purpose MC toolkit was used for simulation which allows to simulate particle-matter interactions [32]. The simulations included physical and chemical stages of radiation to assess the impact of photon energy, the atomic number of NPs, and the characteristics of coatings on dose distributions and radiolysis yields. In the physical stage, the The G4EmLivermorePhysics constructor, configured with a secondary particle production threshold of 100 eV, was utilized for the NPs, while the G4EmDNAPhysics-option2 constructor was employed for the surrounding water medium [33]. A step size limit of 1 nm was implemented, and a complete de-excitation cascade involving Auger and fluorescence interactions was activated, with the energy cutoff disabled for the cascade. For the chemical simulations, the G4EmDNAChemistry-option1 chemistry constructor was chosen [33] and key reactive species generated from water radiolysis, including e_{aq}^{-}, $^{\bullet}OH$, $H^{\bullet}$, H_3O^+, H_2, OH^-, and H_2O_2 were scored for an

interval from 1 ps up to 1 μs. In Geant4-DNA chemistry, the interaction of eV energy electrons, encompassing diffusion, reactions, and the recombination of reactive species resulting from secondary particles, is comprehensively modeled as described by Karamitros et al. [32].

The simulated geometry comprised a single spherical structure NPs (diameter=50 nm) of gold (Au), bismuth (Bi), iridium (Ir), and gadolinium (Gd) were immersed in liquid water phantom ($10\times10\times10$ mm^3) and three distinct mono-energetic photon beams of 30, 60, and 100 keV were simulated. Radial (DEF) were calculated up to a distance of 4 μm from the surface of the NPs. The parallel photon beam was confined to the volume of the nanoparticle coating to ensure that only secondary particles were recorded [33, 34], as depicted in Fig. 1. Dose distribution was recorded in spherical shells with logarithmic thicknesses extending from the NP or coating surface up to a distance of 4 μm, as shown in Fig. 1. The dose enhancement factor ($DEF=D_{\text{with nanoparticle}}/D_{\text{without nanoparticle}}$) [35] and radiolysis enhancement factor ($REF=Y_{\text{with nanoparticle}}/Y_{\text{without nanoparticle}}$) are characterized as the ratio of the deposited dose to the overall quantity of reactive species produced respectively, with and without NP [33, 34].

The effect of nanoparticle coatings on DEF and REF was evaluated by polyethylene glycol (PEG 400(Density: 1.13 g/cm^3, Molar mass: 380–420 g/mol) for bismuth, gold, iridium and gadolinium NPs with thicknesses of 5 and 10 nm (Fig. 2). PEG 400 is widely used in a variety of pharmaceutical formulations. In the simulations for the PEG coatings, a uniform coating was applied, representing various thicknesses while maintaining a consistent coating density [36, 37].

Between 10^5 and 10^6 incident photons were run, chosen based on the radiation stage to optimize computation time while effectively reducing statistical uncertainty.

Results and discussion

Figure 3 shows the calculated secondary particle number emitted from the coated and noncoated NPs exposed by 30, 60, and 100 keV photons. For gold, bismuth, gadolinium, and iridium NPs the maximum values of the secondary particle per initial photon is related to the photons of 30 keV and the minimum secondary particle per initial

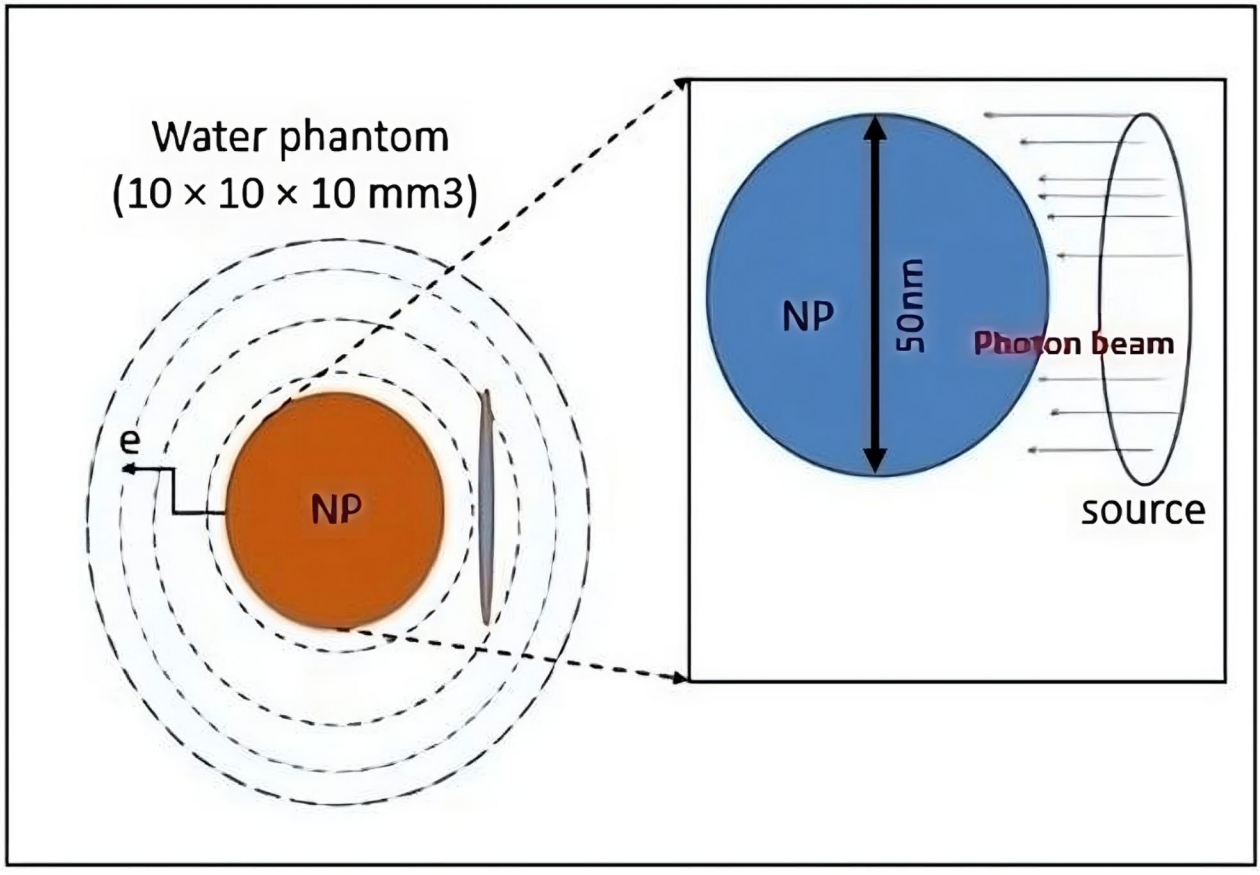

Fig. 1 A schematic diagram illustrates the simulation geometry and the scoring spherical shells (mesh) used to calculate the dose enhancement factor (DEF) around the nanoparticle. The parallel photon beams (in green) are generated from a source positioned near the nanoparticle, while the tracks of secondary electrons (in red) traverse through the 50-nm nanoparticle and the surrounding water medium

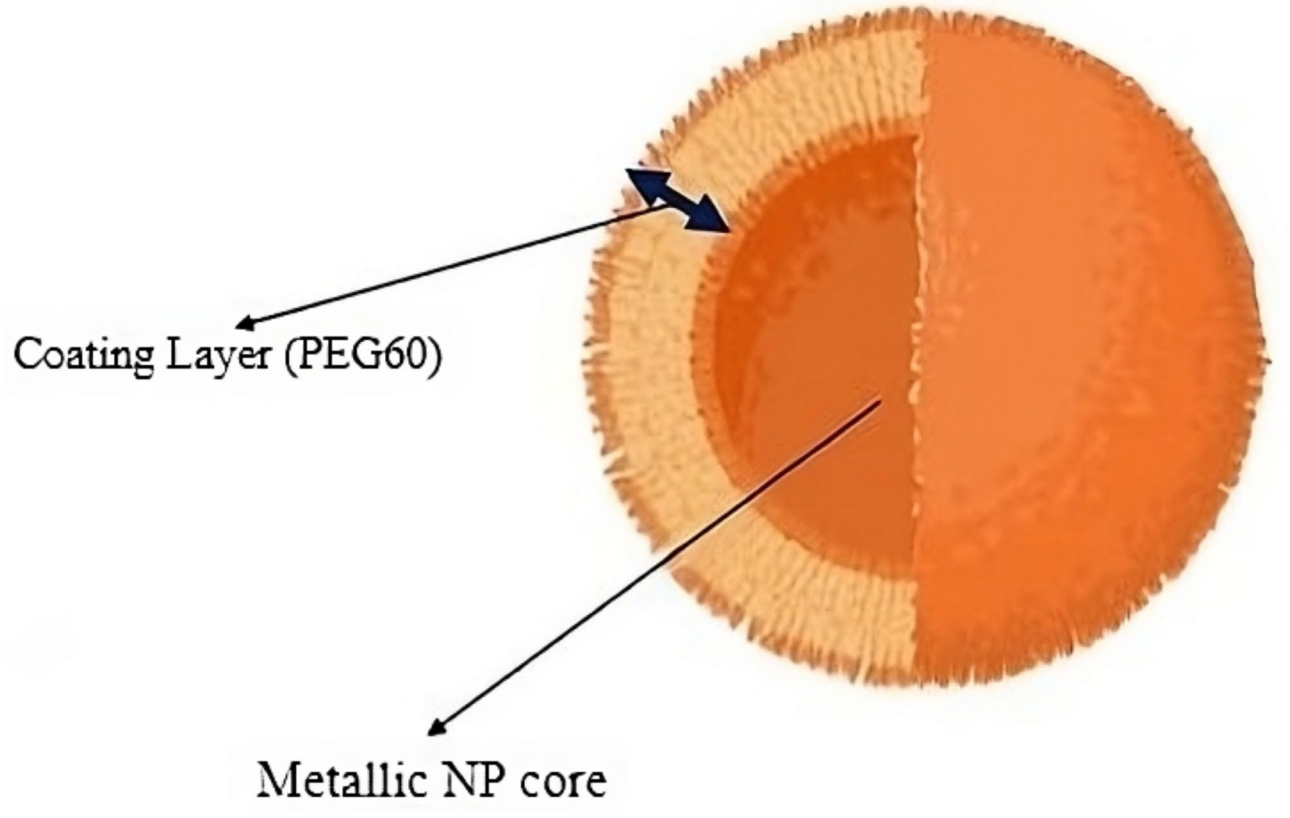

Fig. 2 PEG coated metallic NPs

photon is related to the photons of 60 keV. While, for gadolinium NP, the maximum values of sdthe secondary particle per initial photon is related to the photons of 60 keV. The minimum secondary particle per initial photon is related to the photons of 100 keV. Also, the results show that the coating of NPs leads to decrease in secondary particle per initial photon values for all NPs in all energies. Actually, the number of secondary particles.

generated per initial photon decreases as the thickness of the coating layer increases. The difference between the results of gadolinium and other NPs is due to the difference in K-edge energy of them. The photons of 30 and 100 keV have the energy close to the L- and K-edge energy of the gold, bismuth and iridium NPs and because of that the number of secondary electrons are higher than that of 60 keV. In contrary, for gadolinium NP the 60 keV photon is close to the K-edge of it and because of that the maximum electron number is attributed to the 60 keV. Under keV photon irradiation, the PEG shell can modify the spectrum of low-energy secondary electrons generated from coated gold NPs [36, 38–40]. Li et al. [3] noted that gold NPs exposed to 50 keV X-rays showed that the probability of Auger electron emission from gold in the M shell is 98% greater than that in the N shell, with 33% of the emitted electrons possessing energies between 200 and 300 eV. Auger electrons within this energy range primarily deposit their energy over a distance of approximately 10 nm and can be effectively absorbed by the coating layers. Belousov et al. [39] showed that the coating of gold NP with PEG can influence the amount and the energy spectra of secondary electrons originated from the irradiated gold core. In silico results of Hespeels et al. [41] indicated that the presence of a coating on gold NPs leads to a diminished yield of emitted electrons. Xiao et al. [42] demonstrated that coatings can significantly reduce the emission of low-energy, short-range electrons from gold nanoparticles, resulting in a decreased potential for radiosensitization.

Figure 4 illustrates the dose enhancement factor (DEF) measured for 30, 60, and 100 keV photon beams as a function of the radial distance from the surface of the NPs. The DEF was normalized to 1. The aim was to show the difference between the DEF for NPs with different coating layer thickness and nanoparticle without coating layer. It is clear that DEF values decease as the radial from nanoparticle surface increases. It is obvious that increase of thickness of nanoparticle coating leads to decrease of DEF values. For gold, bismuth and iridium NPs, the DEF values decrease as the incident photon energy increases. But for gold nanoparticle the maximum DEF is related to the 60 keV photons. The difference between the results of gadolinium and other NPs is due to the difference in

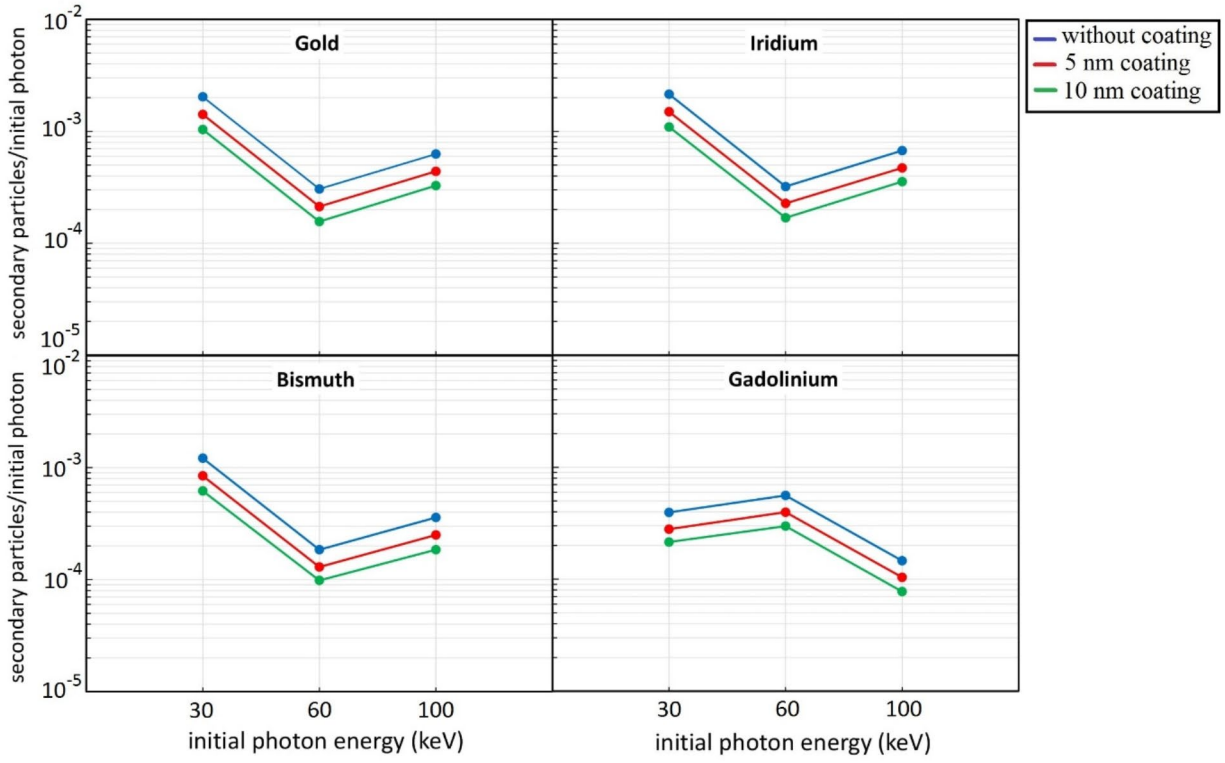

Fig. 3 The overall count of secondary particles (with a statistical uncertainty of under 1%) generated around nanoparticles of gold, bismuth, gadolinium, and iridium when exposed to 30, 60, and 100 keV photon beams

K-edge energy of them. Numerous Monte Carlo studies have demonstrated that, upon exposure to low-energy photons, a significant portion of the dose is deposited within the initial few nanometers surrounding high-Z metallic nanoparticles [26, 43]. The presence of metallic NPs instead of water leads to significant increase in production of low energy and short-range electrons which leads to an increased dose enhancement factor (DEF) extending up to approximately 2 μm from the surface of the NP. Kroger et al. [44] found that coating thickness significantly influenced dose attenuation, with this effect being more pronounced for smaller NPs and higher concentrations. The penetration distance of Auger and Coster–Kronig electrons ranges from nanometers to micrometers in water or tissue, resulting in substantial dose enhancement and a relative biological effectiveness greater than 1 at the cellular level. Peukert et al. [36] indicated that thicker coatings on nanoparticles result in a reduction of the dose enhancement effect.

Figure 5 demonstrates the effect of reactive species generated from water radiolysis in the vicinity of gold, bismuth, gadolinium, and iridium nanoparticles irradiated with 30, 60, and 100 keV incident photons. For gold, bismuth, and iridium NPs the maximum values of REF is related to the photons of 30 keV and minimum REF value is related to the photons of 60 keV. While, for gadolinium NP, the maximum values of REF is related to the photons of 60 KeV and minimum REF value is related to the photons of 100 keV. For gold, bismuth and Iridium NPs under 30 keV REF decrease by coating of NP and increasing the thickness of coating layer and for 100 keV REF is increased by coating of NP and increasing the thickness of coating layer. Difference is not considerable for 60 keV. Coating of NPs have opposite effect on chemical enhancement for 30 keV and 100 keV. Coating layer has a positive physicochemical effect for PEG-coated metallic NPs under 100 keV photons.

The presence of NPs has been associated with increased radical production, even in the absence of radiation [45]. Water is a primary component of cells and serves as the main target for photons. The generated photoelectrons and Auger electrons traverse the cell, interacting with water molecules and resulting in the production of free radicals through hydrolysis. The interaction of produced free radicals with DNA results in DNA damage, ultimately leading to cell death. The water content within the coating, particularly near the surface of the metal core, plays a crucial role in the production of hydroxyl radicals [46]. Haume et al. [46]. indicated that the thickness and water content of the coating layer can significantly affect

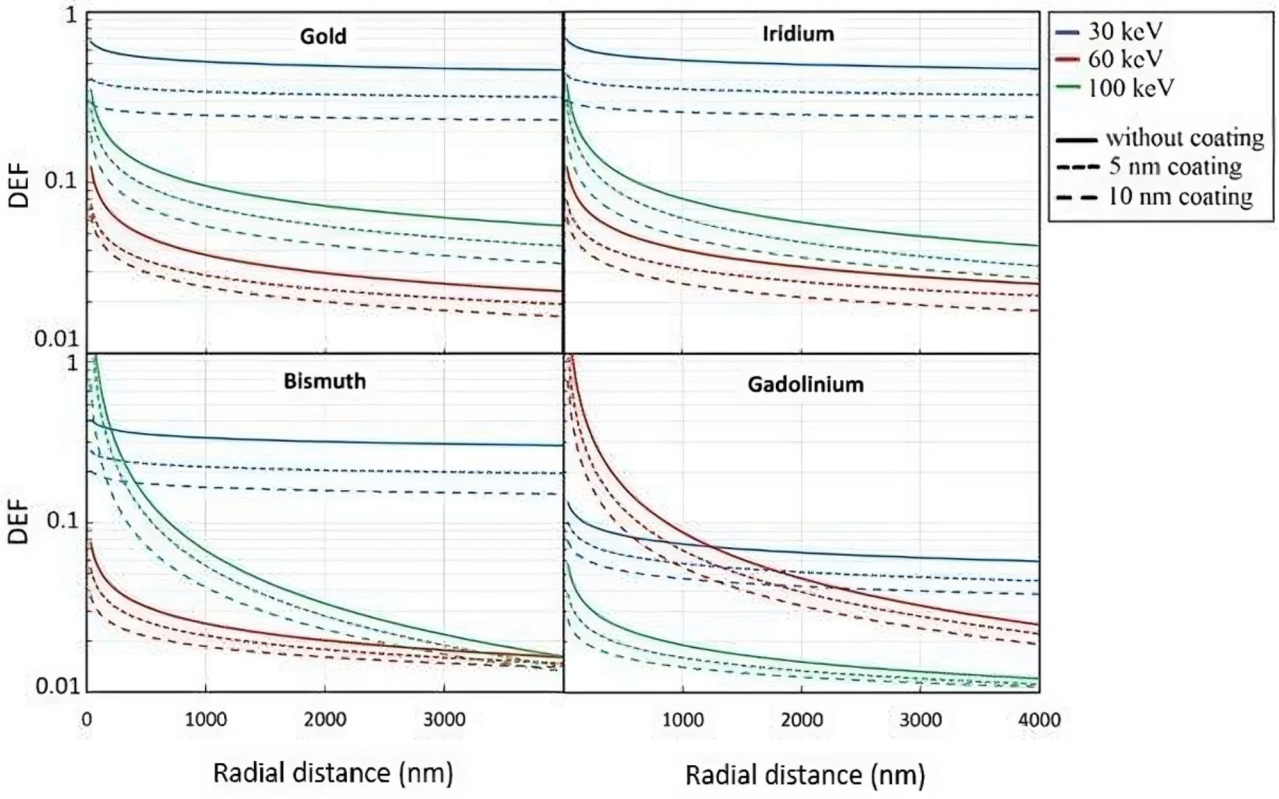

Fig. 4 The DEF calculated for 30, 60, and 100 keV photon beams as a function of radial distance (nm) from the surface of the nanoparticles

the radiosensitization potential of coated NPs. In the study by Haume et al. [46]. the yield of hydroxyl radicals was reduced by six-fold for PEG-coated gold nanoparticles compared to their uncoated counterparts. Dense coatings have low water content and it may influence the radical production [46]. Liu et al. [47] reported the 2–45% decrease in the percentage of surviving cells for murine breast cancer EMT-6 and colon carcinoma CT26 cells exposed to the radiation in presence of gold NPs coated with PEG. Zhang et al. [48] indicated that PEG-coated gold NPs can significantly decrease the cancer cell survival after radiation with gamma-rays. In the study of Peukert et al. [36], it was indicated that an increase in the PEG coating density enhances the effectiveness of the coating while having only a minimal impact on the overall enhancement. Kong et al. [49] demonstrated that breast cancer cells exposed to 200 kVp photons exhibited increased cell death in the presence of gold NPs coated with thioglucose, compared to uncoated gold NPs. Kaur et al. [50] indicated that the exposure of glucose-coated gold NPs in HeLa cells to a ^{60}Co source emitting 1173 keV and 1332 keV photons resulted in the generation of more Compton electrons, leading to increased radiolysis and DNA damage. Additionally, they demonstrated a 29% dose reduction in HeLa cells treated with glucose-coated gold NPs compared to those without such treatment. Gilles et al. [51] showed that for same thickness of PEG layer, the denser PEG (1000Da Vs. 400 Da) suppresses the radical production.

Conclusion

Many simulation studies exploring the radiosensitization potential of NPs have overlooked the significance of their coating layers. This paper investigates the physical and radiobiological effects of metallic NP coatings in nanoparticle-based radiation therapy. Utilizing Geant4 simulations on single NP exposed to keV photons, we found that under low-energy photon irradiation, the coating layer functions as a shield, absorbing low-energy electrons and consequently reducing local and nanoscopic dose enhancement. Given the short range of these electrons, it is advisable that the coating layer thickness not exceed 10–15 nm. Conversely, our results indicate that for PEG-coated metallic NPs under high-energy photon exposure, the coating layer exhibits beneficial physicochemical properties. This dual behavior of the coating layer should be taken into account during the design of NPs and warrants further investigation in future studies.

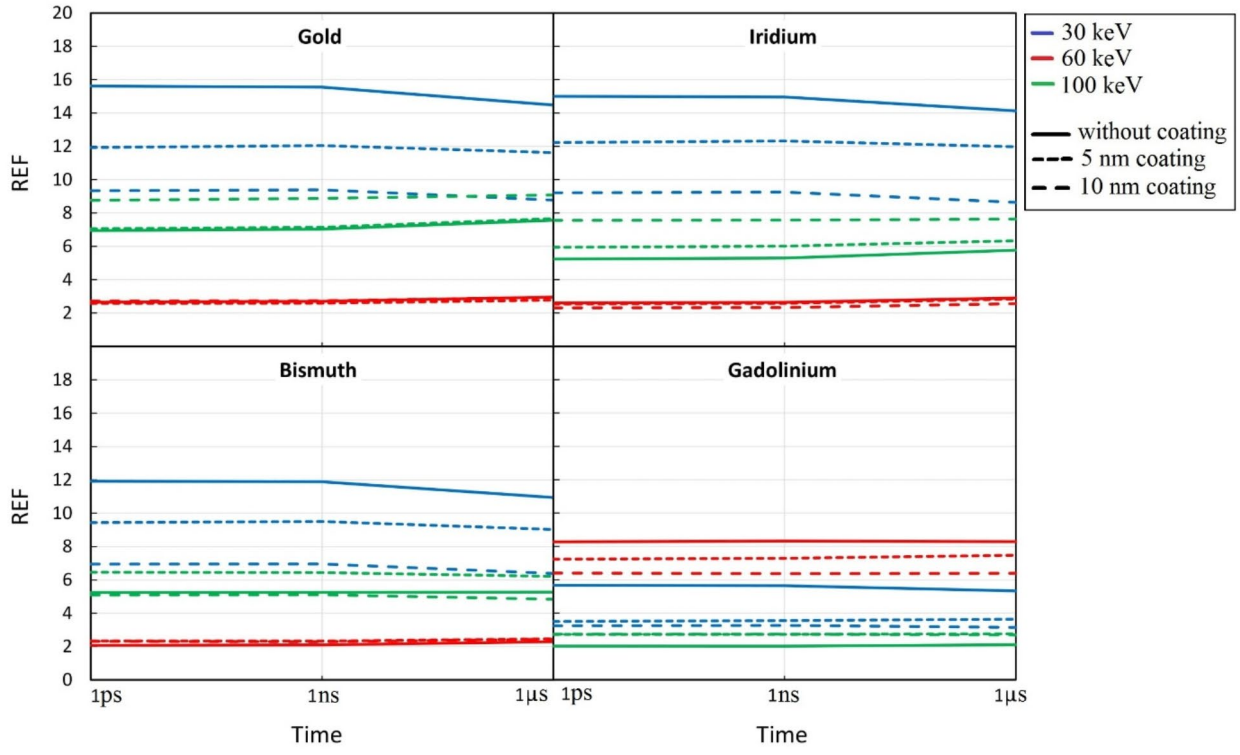

Fig. 5 The effect of reactive species generated from water radiolysis in the vicinity of gold, bismuth, gadolinium, and iridium nanoparticles exposed to 30, 60, and 100 keV incident photons

Abbreviations

MC	Monte Carlo
REF	Reactive Oxygen Species Enhancement Factor
DEF	Dose Enhancement Factor
PEG	Polyethylene Glycol
KV	kilovolt
MV	Mega Volt
NP	Nanoparticle

Acknowledgements
This investigation was supported by Student Research Committee of Tabriz University of Medical Sciences funds (68865/ IR.TBZMED.VCR.REC.1401.010).

Author contributions
The core idea of this study came from Elham Mansouri and Asghar Mesbahi. They also directed Saeed Rajabpour and did the research. Elham Mansouri and Saeed Rajabpour performed the simulation and analyzed the data. Elham Mansouri wrote the manuscript. Final editing was performed by Asghar Mesbahi. All authors have read and agreed to the publishe this version of the manuscript.

Funding
No funding.

Data availability
The datasets used and/or analyzed during the current study are available from the corresponding author on reasonable request.

Declarations

Ethics approval and consent to participate
Not applicable (NA).

Consent for publication
Not applicable (NA).

Competing interests
The authors declare no competing interests.

Received: 2 March 2024 / Accepted: 11 October 2024
Published online: 22 October 2024

References

1. Siddique S, Chow JCL. Gold NPs for Drug Delivery and Cancer Therapy. Appl Sci. 2020;10. https://doi.org/10.3390/app10113824.
2. Moore J, Chow J. Recent progress and applications of gold nanotechnology in medical biophysics using artificial intelligence and mathematical modeling. Nano Express, 2021. 2.
3. Li WA-O et al. Application of High-Z gold NPs in targeted Cancer Radiotherapy-Pharmacokinetic modeling, Monte Carlo Simulation and Radiobiological Effect modeling. LID – 10.3390/cancers13215370 LID – 5370 2021(2072–6694 (Print)).
4. Salado-Leza D et al. Radio-Enhancing properties of bimetallic au:pt NPs: experimental and theoretical evidence. Int J Mol Sci, 2019. 20(22).
5. Lazaro-Carrillo A, et al. Tailor-made PEG coated iron oxide NPs as contrast agents for long lasting magnetic resonance molecular imaging of solid cancers. Mater Sci Engineering: C. 2020;107:110262.
6. Xu W, et al. Tailored synthesis of PEGylated Bismuth NPs for X-ray computed Tomography and Photothermal Therapy: One-Pot, targeted pyrolysis, and Self-Promotion. ACS Applied Materials & Interfaces; 2020.
7. Mansouri E, Mesbahi A, Yazdani P. Analysis of physical dose enhancement in nano-scale for nanoparticle-based radiation therapy: a cluster and endothelial cell model %J. Nanomed J. 2021;8(1):30–41.

8. Polf JC, et al. Enhanced relative biological effectiveness of proton radiotherapy in tumor cells with internalized gold NPs. Appl Phys Lett. 2011;98(19):193702.
9. Li F, et al. Radiosensitizing Effect of Gadolinium Oxide nanocrystals in NSCLC cells under Carbon Ion Irradiation. Nanoscale Res Lett. 2019;14(1):328.
10. Mesbahi A, Mansouri E, Mohammadzadeh M. Nanoscale dosimetric consequences around bismuth, gold, gadolinium, hafnium, and iridium NPs irradiated by low energy photons. Pol J Med Phys Eng. 2020;26(4):225–34.
11. Robatjazi M, et al. Monte Carlo-based calculation of nano-scale dose enhancement factor and relative biological effectiveness in using different NPs as a radiosensitizer. Int J Radiat Biol. 2021;97(9):1289–98.
12. Peukert D, et al. Gold nanoparticle enhanced Proton Therapy: Monte Carlo modeling of reactive species' distributions around a gold nanoparticle and the effects of Nanoparticle Proximity and Clustering. Int J Mol Sci. 2019;20(17):4280.
13. Rasouli FS, Masoudi SF. Monte Carlo investigation of the effect of gold NPs' distribution on cellular dose enhancement. Radiat Phys Chem. 2019;158:6–12.
14. Kirill M, et al. Radiosensitization by Gold NPs: impact of the size, dose rate, and Photon Energy. Nanomaterials. 2020;10:952.
15. Jones BL, Krishnan SH, Fau - S, Cho, Cho SH. Estimation of microscopic dose enhancement factor around gold NPs by Monte Carlo calculations. (0094-2405 (Print)).
16. Huynh NH, Chow JCL. DNA dosimetry with Gold Nanoparticle irradiated by Proton beams: a Monte Carlo Study on Dose Enhancement. Appl Sci. 2021;11. https://doi.org/10.3390/app112210856.
17. Santiago CA. Chow variations in gold nanoparticle size on DNA damage: a Monte Carlo Study based on a multiple-particle model using Electron beams. Appl Sci. 2023;13. https://doi.org/10.3390/app13084916.
18. James CLC. Recent progress in Monte Carlo simulation on gold nanoparticle radiosensitization. AIMS Biophys. 2018;5(4):231–44.
19. Chow J. Recent progress in Monte Carlo simulation on gold nanoparticle radiosensitization. AIMS Biophys. 2018;5:231–44.
20. Ekinci F et al. Analysing the effect of cranium thickness on Bragg peak range in Proton Therapy: a TRIM and GEANT4 based study. St Petersburg Polytechnical Univ Journal: Phys Math, 2022. 15.
21. Ekinci F, et al. MC TRIM algorithm in Mandibula Phantom in Helium Therapy. Healthcare. 2023;11. https://doi.org/10.3390/healthcare11182523.
22. Ekinci F. Investigation of tissue equivalence of phantom biomaterials in 4He heavy ion therapy. Radiat Eff Defects Solids. 2023;178(3–4):500–9.
23. Klapproth AP, et al. Multi-scale Monte Carlo simulations of gold nanoparticle-induced DNA damages for kilovoltage X-ray irradiation in a xenograft mouse model using TOPAS-nBio. Cancer Nanotechnol. 2021;12(1):27.
24. Lechtman E, Pignol J-P. Interplay between the gold nanoparticle sub-cellular localization, size, and the photon energy for radiosensitization. Sci Rep. 2017;7(1):13268.
25. Leung MK et al. Irradiation of gold NPs by x-rays: Monte Carlo simulation of dose enhancements and the spatial properties of the secondary electrons production. Med Phys, 2011(0094-2405 (Print)).
26. McMahon SJ, et al. Nanodosimetric effects of gold NPs in megavoltage radiation therapy. Radiother Oncol. 2011;100(3):412–6.
27. Liu R, et al. Development of computational model for cell dose and DNA damage quantification of multicellular system. Int J Radiat Biol. 2019;95(11):1484–97.
28. Gray T, et al. A detailed experimental and Monte Carlo analysis of gold nanoparticle dose enhancement using 6 MV and 18 MV external beam energies in a macroscopic scale. Appl Radiat Isot. 2021;171:109638.
29. Ekinci FA-O, Acici KA-O, Asuroglu TA-O. Enhancing tissue equivalence in (7)Li Heavy Ion Therapy with MC Algorithm Optimized Polymer-based Bioinks. LID – 10.3390/jfb14120559 [doi] LID – 559. J Funct Biomater, 2023. 14(12).
30. Ekinci F, Aşlar E. Thyroid and contralateral breast surface dose variation in mammography: a phantom study on the role of breast tissue composition. Eur Phys J Plus. 2024;139(4):330.
31. Vinković Vrček I, et al. Does surface coating of metallic NPs modulate their interference with in vitro assays? RSC Adv. 2015;5(87):70787–807.
32. Sakata D, et al. Electron track structure simulations in a gold nanoparticle using Geant4-DNA. Physica Med. 2019;63:98–104.
33. Tran HN, et al. Geant4 Monte Carlo simulation of absorbed dose and radiolysis yields enhancement from a gold nanoparticle under MeV Proton irradiation. Nucl Instrum Methods Phys Res Sect B. 2016;373:126–39.
34. Rajabpour S, et al. Comparing Geant4 physics models for proton-induced dose deposition and radiolysis enhancement from a gold nanoparticle. Sci Rep. 2022;12(1):1779.
35. Sheeraz Z, Chow JCL. Evaluation of dose enhancement with gold NPs in kilovoltage radiotherapy using the new EGS geometry library in Monte Carlo simulation. AIMS Biophys. 2021;8(4):337–45.
36. Peukert D, et al. Gold nanoparticle enhanced proton therapy: a Monte Carlo simulation of the effects of proton energy, nanoparticle size, coating material, and coating thickness on dose and radiolysis yield. Med Phys. 2020;47(2):651–61.
37. Sebby KB, Mansfield E. Determ Surf Density Polyethyl Glycol gold NPs use Microscale Thermogravimetric Anal 2015(1618–2650 (Electronic)).
38. Terekhin VV, et al. Conjugates of gold NPs and poly(ethylene glycol): formation in hydrosol, direct transfer to organic medium, and stability of organosols. Colloid J. 2015;77(4):511–9.
39. Belousov AV, et al. Spectra of secondary particles generated upon virtual irradiation of gold nanosensitizers: implications for surface modification. Biomedical Phys Eng Express. 2018;4(4):045023.
40. Spaas C, et al. Dependence of Gold Nanoparticle Radiosensitization on Functionalizing Layer Thickness. Radiat Res. 2016;185(4):384–92.
41. Félicien H et al. Experimental measurements validate the use of the binary encounter approximation model to accurately compute proton induced dose and radiolysis enhancement from gold NPs. Phys Med Biol, 2019. 64.
42. Xiao F, et al. On the role of low-energy electrons in the radiosensitization of DNA by gold NPs. Nanotechnology. 2011;22(46):465101–465101.
43. Zygmanski P, Sajo E. Nanoscale radiation transport and clinical beam modeling for gold nanoparticle dose enhanced radiotherapy (GNPT) using X-rays. Br J Radiol. 2016;89(1059):20150200.
44. Koger B, Kirkby C. Dosimetric effects of polyethylene glycol surface coatings on gold nanoparticle radiosensitization. Phys Med Biol. 2017;62(21):8455–69.
45. Rosa S, et al. Biological mechanisms of gold nanoparticle radiosensitization. Cancer Nanotechnol. 2017;8(1):2.
46. Haume K, et al. Gold NPs for cancer radiotherapy: a review. Cancer Nanotechnol. 2016;7(1):8–8.
47. Liu CJ, et al. Enhancement of cell radiation sensitivity by pegylated gold NPs. Phys Med Biol. 2010;55(4):931–45.
48. Zhang X-D, et al. Size-dependent radiosensitization of PEG-coated gold NPs for cancer radiation therapy. Biomaterials. 2012;33(27):6408–19.
49. Kong T, et al. Enhancement of Radiation cytotoxicity in breast-Cancer cells by localized attachment of gold NPs. Small. 2008;4(9):1537–43.
50. Kaur H, et al. In vitro studies on radiosensitization effect of glucose capped gold NPs in photon and ion irradiation of HeLa cells. Nucl Instrum Methods Phys Res Sect B. 2013;301:7–11.
51. Gilles M, Brun E, Sicard-Roselli C. Gold NPs functionalization notably decreases radiosensitization through hydroxyl radical production under ionizing radiation. Colloids Surf B. 2014;123:770–7.

Publisher's note